Evaluation of black carbon emission inventories using a Lagrangian dispersion model- a case study over Southern India

H. S. Gadhavi[1], K. Renuka[1], V. Ravi Kiran[1], A. Jayaraman[1], A. Stohl[2], Z. Klimont[3] and G. Beig[4]

[1]{National Atmospheric Research Laboratory, Gadanki, 517 112, India}

[2]{Norwegian Institute for Air Research, Instituttveien 18, 2027 Kjeller, Norway}

[3]{International Institute for Applied Systems Analysis, A-2361 Laxenburg, Austria}

[4]{Indian Institute of Tropical Meteorology, Dr. Homi Bhabha Road, Pashan, Pune, 411 004, India}

Correspondence to: H. S. Gadhavi (harish.gadhavi@gmail.com; harish@narl.gov.in)

Abstract

We evaluated three emission inventories of black carbon (BC) using Lagrangian particle dispersion model simulations and BC observations from a rural site in Southern India (Gadanki; 13.48° N, 79.18° E) from 2008 to 2012. We found that 93% to 95% of the BC load at the observation site originated from emissions in India and the rest from the neighbouring countries and shipping. A substantial fraction (33% to 43%) of the BC was transported from Northern India. Wet deposition is found to play a minor role in reducing BC mass at the site because of its proximity to BC sources during rainy season and relatively short rainy season over western and northern parts of India. Seasonally, the highest BC concentration (approx. 3.3 μg/m^3) is observed during winter, followed by spring (approx. 2.8 μg/m^3). While the model reproduced well the seasonal cycle, the modelled BC concentrations are significantly lower than observed values, especially in spring. The model bias is correlated to fire radiative power – a proxy of open biomass burning activity. Using potential emission sensitivity maps

derived using the model, we suggest that underestimation of BC mass in the model during spring is due to the underestimation of BC fluxes over Southern India (possibly from open-biomass-burning/forest-fires). The overall performance of the model simulations using three different emission inventories (SAFAR-India, ECLIPSE and RETRO) is similar, with ECLIPSE and SAFAR-India performing marginally better as both have about 30% higher emissions for India than RETRO. The ratio of observed to modelled annual mean BC concentration was estimated as 1.5 for SAFAR, 1.7 for ECLIPSE and 2.4 for RETRO.

1 Introduction

Black carbon (BC) is a component of soot, which is responsible for the absorption of visible light (Yasa et al., 1979). It is emitted into the atmosphere as a consequence of incomplete combustion processes like biofuel burning, running of inefficient diesel engines, forest fires, etc. Unlike other aerosols, BC aerosols are responsible for positive radiative forcing which is comparable to forcing by major greenhouse gases (Haywood and Ramaswamy, 1998; Jacobson, 2001; Bond et al., 2013). Presence of BC in the atmosphere also affects the hydrological cycle of Earth and regional climate (Ackerman et al., 2000).

Understanding the sources of BC, their geographical distribution and future changes is therefore important to improve climate modelling and would support development of policies exploring climate co-benefits of air pollution regulation controlling sources of BC. However, global BC emissions estimates are highly uncertain. Dickerson et al. (2002) estimated BC emissions of South Asia between 2 and 3 Tg in year 1999 using BC/CO ratio which were factor of 2 to 3 higher than bottom-up BC inventories suggesting significant underestimation of BC sources in South Asia. The range of global BC emissions has been reported as 4 to 13 Tg/yr (Bond et al., 2013). Emissions from India contribute 7% to 14% of global BC emissions (Bond et al., 2004; Schultz and Rast, 2007; Klimont et al., 2009; Klimont et al., 2015a, b) and observed BC concentrations over India are significantly higher than in other regions (Suresh Babu and Moorthy, 2002; Suresh Babu et al., 2002; Ganguly et al., 2005; Ganguly et al., 2006a, b; Jayaraman et al., 2006; Ramachandran and Rajesh, 2007; Beegum et al., 2009; Gadhavi and Jayaraman, 2010; Ramachandran and Kedia, 2010; Vinoj et al., 2010; Raghavendra Kumar et al., 2011). Model predicted BC concentrations over India are

generally found to be factor of two to six lower than those observed (Ganguly et al., 2009; Nair et al., 2012; Bond et al., 2013; Moorthy et al., 2013). This raises the question whether the observed high BC concentrations over India are the result of transport from other places, relatively inefficient removal of BC compared to elsewhere, or underestimation of emissions from India.

In this article we examine the emission inventories RETRO (Schultz et al., 2007; Schultz and Rast, 2007), ECLIPSE (Klimont et al., 2013; Klimont et al., 2015a, b) and SAFAR-India (Sahu et al., 2008) using the particle dispersion model FLEXPART (Stohl et al., 1998; Stohl et al., 2005) driven by observed meteorological fields and suggest possible causes of the underestimation of BC concentrations by models over India.

2 Site Description

Observations of BC have been carried out at the climate observatory of the National Atmospheric Research Laboratory in Gadanki. Gadanki (13.48° N and 79.18° E, 365 m above mean-sea-level) is a typical rural site in southern India, with no major industrial activities in the near vicinity. Gadanki has tropical wet climate and experiences a prolonged rainy season from both south-west and north-east monsoons unlike the northern and western parts of India. Monthly rainfall patterns over Gadanki for the years 2009 and 2011 are shown in Fig. 1. February to May is mostly dry. The rainy season starts in June and goes on until December with short lulls in between. The maximum rainfall over Gadanki in the year 2009 was observed during November whereas in the year 2011 it occurred during August with a comparable rain amount in November. The year 2009 was officially declared as a drought year for the state of Andhra Pradesh (in which Gadanki is located), whereas 2011 was a normal year.

Open biomass burning has a well characterized seasonal cycle over India (Joseph et al., 2009). Fire radiative power (FRP) is a measure of radiative energy emitted per unit time in a fire event. Its value is proportional to amount of material being burnt in the fire event. Fires detected using MODIS satellite sensor are characterised by FRP values using an empirical formula based on difference in brightness temperature at 4 μm with respect to non-fire pixels in the vicinity (Giglio et al., 2003; Justice et al., 2006; Davies et al., 2009). In Figure 2, long-term (2000-2013) monthly median FRP values over the southern part of India (south of 18° N

latitude; henceforth referred as Peninsular India) and over whole of India are shown. FRP is high during February to May and low during June to September. The largest differences in the seasonal variation of FRP between Peninsular India and whole India occur during October to November. As mentioned before, Peninsular India where the observations are carried out experiences two rainy-seasons whereas North, West and Central India experiences only one rainy-season. The North-East monsoon brings rain over Peninsular India during winter and reduces the number of fire events and hence FRP whereas absence of rain results in high FRP over other parts of India.

3 Instrumentation and Data

Equivalent BC (EBC) concentrations are measured using an aethalometer (Model AE31; Magee-Scientific, USA), which has 7 wavelength channels centred at 370, 470, 520, 590, 660, 880 and 950 nm. In this study, we report EBC values based on 880 nm channel data as it has minimum interference from other species and is considered to be the standard channel for BC measurement with this technology (Hansen, 2005). Details of the instrument and the typical set-up used at Gadanki are reported in an earlier study (Gadhavi and Jayaraman, 2010). The ambient air is drawn with a typical flow rate of 2.9 litres per minute for five minutes and passes through a quartz fibre filter fitted in an optical chamber. Changes in transmission of light through filter paper is monitored which is affected by accumulated deposition of light absorbing particles on the filter paper. The changes in absorption coefficient of filter paper are converted to equivalent BC mass by dividing it with mass absorption cross-section 0.166 $cm^2/\mu g$ (at 880 nm). Assuming that most of light absorption is due to BC at 880 nm, for the convenience of comparisons with the model simulations, we refer to these measurements as BC. The error in estimating BC concentration is expected to be less than 10% (Hansen, 2005; Gadhavi and Jayaraman, 2010 and references therein).

3.1 Emission Inventory Data

We have considered three emission inventories namely ECLIPSE, RETRO and SAFAR-India. The ECLIPSE (Evaluating the CLimate and air quality ImPacts of Short-livEd pollutants) global emission inventory has been developed using the GAINS Model (Greenhouse gas – Air pollution Interactions and Synergies Model; Amann et al. (2011)). The sources considered

range from wick lamps to thermal power stations, including residential combustion, transport, shipping, large combustion installations, industrial processes, waste and open burning of agricultural residues. This inventory does not include emissions from open biomass burning other than agricultural waste burning. Hence forest-fire emissions are included from GFEDv3 (Global Fire Emissions Database; van der Werf et al. (2010)). ECLIPSE emission dataset has been developed for the period from 1990 to 2050; the inventory extends to 2010 while the baseline projection until 2050 assumes implementation of existing environmental legislation and draws on the energy projection of IEA (International Energy Agency's Energy Technology Perspective – 2012 (ETP2012))(Klimont et al., 2015a, b). In this work, emission values for the year 2010 from version 5 of the inventory are used. Version 5 was recently released and has about 44% higher emissions than version 4a inventory over India, mainly due to addition of sources which are not previously considered (e.g. wick lamps). The original data-set is available at 0.5° x 0.5° resolution including monthly resolution for several key source sectors; however in this study, the grid resolution has been reduced to 1° x 1°. Emission fluxes from the ECLIPSE + GFED inventory are shown in Fig. 3a. Hereafter, if not specifically mentioned, reference to ECLIPSE inventory implies ECLIPSE + GFED. The total BC emissions of India in 2010 are estimated at 1233 Gg/yr of which 52 Gg/yr are from forest fire emissions based on GFED. Major contribution originates from the Indo-Gangetic Basin (IGB) in the north and in a few pockets on the western coast of India. In contrast, in South and Central India BC emissions are relatively low. Within IGB, emissions are higher in Bihar, West Bengal and Haryana states of India and Bangladesh (a map of India with state names is provided in supporting material).

The RETRO emission inventory is the outcome of the project REanalysis of the TROpospheric (RETRO) chemical composition over the past 40 years. The emission inventory for BC has two parts – one for anthropogenic emissions which includes biofuel burning, industrial combustion and agricultural residue burning. BC emissions from forest fires over India are accounted for separately based on the Reg-FIRM model (Schultz et al., 2008). Schultz et al. (2008) had to reduce the literature values for carbon emissions per unit area over India to achieve consistency with reported emissions from the subcontinent which highlights inherent problems in the bottom-up inventory approach for emissions from biomass burning. The emission fluxes are monthly averages of BC in $kg/m^2/s$ for each grid box.

Annual total BC emissions of India based on this inventory for the year 2010 are 697 Gg/yr out of which 31 Gg/yr are from forest fires. In Figure 3b, differences between ECLIPSE and RETRO (ECLIPSE - RETRO) are shown, i.e. RETRO emission fluxes are lower than ECLIPSE emissions in all of South Asia. The difference is particularly high over the Bihar, West Bengal states of India, and Bangladesh and Myanmar.

Finally, we have considered the regional emission inventory SAFAR (System of Air quality Forecasting and Research)-India (Sahu et al., 2008). The SAFAR-India includes only anthropogenic emissions from fossil fuel, fuel wood, dung combustion and agricultural waste burning using district level statistics on activities, population, farming, etc. In preparation of the inventory, Sahu et al. (2008) have used emission factors for bio-fuel combustion from Venkataraman et al. (2005), and emission factors for fossil fuel combustion are based on Cooke et al. (1999) for their "under-developed-countries" category. The inventory was updated after publication of Sahu et al. (2008). The latest inventory contains annual emissions for the years 1991, 2001 and 2011 at a spatial resolution of 1° x 1°. In this work, we have used emission values for 2011. Total BC emissions of India based on this inventory are 1119 Gg/yr. Though ECLIPSE and SAFAR inventory have comparable total emissions for India, their spatial and source distribution are significantly different. In Figure 3c, spatial allocation differences between ECLIPSE and SAFAR (ECLIPSE – SAFAR) are shown. SAFAR inventory has comparable or marginally higher emissions in central, southern and western part of India. Regions close to big cities like Mumbai, Delhi, Ahmedabad and Kolkata have significantly higher emissions in SAFAR compared to ECLIPSE. The opposite is true over Bihar, West Bengal and North Eastern parts of India, where the ECLIPSE inventory is significantly higher than SAFAR. With respect to source distribution, the key difference is between large combustion plants (power plants and industrial boilers) and residential sector. SAFAR estimates large BC emissions from power plant boilers while this source is very small in ECLIPSE. This is linked to the used emission factors, i.e. SAFAR uses values from Cooke et al. (1999) who suggested high emission factors for large industrial boilers but Bond et al. (2004) concluded that there is no evidence for so high values. ECLIPSE relies on smaller values as discussed in Bond et al. (2004) and Kupiainen and Klimont (2007). For residential sector, ECLIPSE includes specific calculation of emissions from diesel generators and wick

lamps; particularly inclusion of the latter source resulted in additional BC emissions leading to higher estimates in the version 5 of ECLIPSE.

3.2 Model Description

We have used the Lagrangian particle dispersion model (LPDM) FLEXPART v9.0 (Stohl et al., 1998; Stohl et al., 2005). The LPDM computes the trajectories of a large number of particles (infinitesimally small air parcels). Unlike ordinary air back trajectory models, FLEXPART includes several processes important for aerosol dispersion and removal like diffusion by turbulence in the boundary layer and aloft, deep convective mixing, dry deposition and wet deposition. The representation of narrow plumes is not possible in Eulerian models whereas in LPDM, one can track the particles correctly at sub-grid scale. Furthermore, FLEXPART can be run in both forward- and backward-in-time modes. The output of the forward modelling from emission sources are simulated concentration fields, whereas a backward run of the model initialized from a receptor point (typically, a measurement location) provides source-receptor (S-R) relationships or potential emission sensitivity (PES) fields. A detailed description about FLEXPART based S-R relationship can be found in Seibert and Frank (2004). It is related to residence time of particles in output grid cells. The S-R relationship describes sensitivity of receptor **y** to source **x**. In the present case, the receptor $\boldsymbol{y}$ is a vector of 24 hour average black carbon concentrations at Gadanki for different days and source $\boldsymbol{x}$ is vector of area averaged black carbon emissions in different grid-boxes at different time intervals. In case of FLEXPART based S-R relationship, the S-R relationship is a matrix $\boldsymbol{M}$ whose elements m_{il} are defined by $m_{il}=\frac{y_l}{x_i}$ (Seibert and Frank, 2004). Once the matrix $\boldsymbol{M}$ is known for a given source vector (emission inventory), receptor values (BC concentrations at measurement site) can be obtained by a simple matrix-vector multiplication. The backward (also known as retroplume) runs are particularly useful to understand the regional distribution of sources contributing to pollution at the observation site and the corresponding transport pathways and for evaluating emission inventories using point observations.

We have used NCEP Global Forecast Systems Final (GFS-FNL; NCEP [2000]; hereinafter referred to as FNL data) meteorological analysis data to drive FLEXPART. GFS-FNL data are available at 1° x 1° spatial resolution and at 6 hourly temporal resolution. Vertically, the data are available at 26 pressure levels extending from the surface to 10 hPa.

We have used backward runs of FLEXPART to simulate the BC concentrations at Gadanki to understand the relative merit of various inventories for the comparison of modelled values with observations. Various settings for the model runs are summarized in Table 1. In the backward runs, BC particles were traced backward in time from the receptor site (Gadanki) for 10 days. The simulations were carried out for every day of the years 2009 and 2011. Since the FNL data do not include precipitation values for the year 2009, the model particles were subjected to only dry deposition in the year 2009 whereas the particles were subjected to both, dry and wet deposition in the year 2011. To calculate dry deposition, particle density, aerodynamic diameter and standard deviation of a log-normal distribution were assumed to be 1400 kg/m^3, 0.25 μm and 1.25, respectively following Stohl et al. (2013). Below-cloud scavenging is modelled using wet scavenging coefficient defined as $\lambda = AI^B$, where A is wet scavenging coefficient at precipitation rate (I) equal to 1 mm/hour, and B is factor dependency (McMahon and Denison, 1979). We have set values of A equal to $2x10^{-7}$ s^{-1} and B equal to 0.62 following Stohl et al. (2013). The in-cloud scavenging is simulated using scavenging coefficient defined as $\lambda=(1.25\ I^{0.64})/H$, where H is cloud thickness in meters (Hertel et al., 1995). The PES values in the bottom most layer (so-called footprint layer; 0-100 m agl) were multiplied by the emission fluxes to calculate the BC concentration at the receptor.

4 Results and discussion

4.1 Observations

Daily mean measured BC concentrations at Gadanki from April 2008 to October 2012 are shown in Fig. 4. BC concentrations at Gadanki vary strongly with season, with high values during late winter and spring and low values during monsoon months. The daily mean values varied from 6.8±3.1 μg/m^3 (February) to 0.3±0.2 μg/m^3 (November). Though the data period is not sufficient to do a thorough trend analysis, for the available data, no trend is observed. Also, there are no major differences in seasonal peak and low concentrations from 2008 to

2012. Hence, keeping computational time constraints in mind, the numerical simulations were carried out only for the relatively dry year 2009 and the normally wet year 2011.

4.2 Potential Emission Sensitivity

The model output is PES values on a three dimensional grid. Since BC is mainly emitted near surface, we focus here only on the PES of the bottom most layer from 0 to 100 m above ground level, the so-called footprint layer and refer to this simply as PES. PES maps for five different days representing different meteorological situations are shown in Fig. 5(a-f). PES maps for all the days during 2009 are provided in the supporting material. PES values are represented in a logarithmic colour scale defined on the side of figure. The median height of the retroplume in daily intervals is shown using gray-shaded dots. Depending on the season, Gadanki receives air coming from different regions. Generally, during winter air parcels are either from the Indo-Gangetic Basin (northern India) or Central Bay of Bengal (e.g. Fig. 5a and 5b). During summer or South West Monsoon period the air comes from the Northern Indian Ocean and Arabian Sea (e.g. Fig. 5c). During the transition period, the air travels over Western and Central India before reaching Gadanki (e.g. Fig. 5d). It is rare that significant PES values occur over South East Asian countries or China, though in few instances trajectories came from Myanmar, South East Asian countries and South China (e.g. Fig. 5b). The advantage of a dispersion model vis-a-vis a simple air trajectory model can be seen in Fig. 5c. The median trajectory shown with grey dots is found to pass over the Arabian Peninsula, though surface PES values are not significant over the Arabian Peninsula, but are substantial over the Northern Indian Ocean. In such circumstances, simple air back-trajectory analysis may ascribe observed concentration to emissions over Arabia whereas in reality it is not being influenced by surface emissions over that region. To demonstrate the effect of wet-deposition on PES, PES maps for 14 October 2011 are shown with and without wet-deposition in Fig. 5e and 5f respectively. The week preceding 14 October 2011 had large rainfall over Southern India and Bay of Bengal. Precipitation maps for 6 days from TRMM satellite are provided in the supporting material. Wet-deposition is generally the most important removal process for aerosol and its effect on PES can be seen by the reduction of the high PES area especially over the ocean. However, the highest PES values over India close to the observation site remain almost unaffected by precipitation. Simulated BC

concentrations for this case with and without precipitation are 1.0 μg/m^3 and 1.4 μg/m^3, respectively.

4.3 Modelled BC Concentrations

BC concentrations are determined by multiplying the footprint PES values with emission fluxes from the various inventories for every grid-point and then integrating over the whole globe. The method implies that BC emissions are uniformly distributed in grid-cell of height 100 m (height of footprint PES layer). For a surface source, the footprint PES layer should be as small as possible. However, a very shallow footprint layer is not ideal from statistical point of view, as the PES is calculated based on the mass (and, thus, approximately the number) of particles in the footprint layer. With a very shallow height (say, 10 m), one would need to release 10 times more particles (number of trajectories) than with a 100 m height of the footprint layer to arrive at the same statistical error for the footprint PES. Whereas increasing the height of PES layer will not introduce significant error as long as the boundary layer height is higher than the footprint PES layer. BC concentrations are calculated with the three emission inventories ECLIPSE, RETRO, and SAFAR-India. The SAFAR-India emission inventory is available only for the Indian region, hence inventory values outside India are set to zero. In case of ECLIPSE inventory, emissions outside India including shipping are found to contribute on average 6% of the total modelled BC concentrations over Gadanki. There were only 36 days in the year 2009 that had more than 15% of the BC originating from emissions outside India. Note that for the year 2009, wet-deposition was not simulated. In case of 2011, for which wet deposition was simulated, emissions outside India contributed 5% on average and there were only 24 days when their contribution was more than 15%. In Figure 6, seasonal and annual averages of source contribution maps are shown. During winter the emissions from IGB region (North India) dominate the BC concentrations at Gadanki, whereas during spring, emissions from Southern India dominate. During summer, the source region is very small resulting in low concentration of BC as shown later. Autumn is a transition period from south-west monsoon to north-east monsoon and hence BC concentrations at Gadanki are due to both Northern and Southern India emissions. On average, India north of 18° N latitude contributes 43% of simulated BC mass and the part

north of 22° N latitude contribute 33% at Gadanki. The contribution increases to 67% and 57% during winter from the two regions, respectively.

A comparison of observed and model estimated BC concentration for the year 2009 is shown in Fig. 7a. There are no big differences between the three emission inventories. BC estimates based on RETRO are a little lower than for the other inventories, as expected, since total BC emissions of India (697 Gg/yr) in RETRO are significantly lower than in the other two inventories. Overall, the seasonal pattern is well reproduced in the model runs. Several sub-monthly scale variations of observed BC concentrations are also well reproduced by the model, confirming its ability to simulate the influence of short-term changes in the meteorological conditions. During autumn and winter, the observed values are reproduced by the model within around 30% but the model underestimates the observed BC concentrations during spring and summer quite substantially. In Table 2, values of annual and seasonal averages, observation to model ratio, mean biases, root mean square differences (RMSD) and correlation coefficients (R) between observation and model for different inventories are shown. Overall, SAFAR has the smallest bias (0.8 $\mu g/m^3$) and least RMSD (1.4 $\mu g/m^3$ in 2009 and 1.1 $\mu g/m^3$ in 2011) with comparable values for ECLIPSE. The bias is small during autumn in general. In fact, with the SAFAR inventory, the model overestimates the observed concentrations during autumn of 2009 by a small amount (0.104 $\mu g/m^3$). The largest bias and RMSD are found during spring. Note, that seasonal variations in model values are purely due to meteorology and transport as emission fluxes are constant within a month in the ECLIPSE and RETRO inventories and throughout the year for SAFAR inventory. Though the SAFAR inventory has seasonally fixed emission fluxes, the model's performance using the SAFAR inventory is not very different compared to using the ECLIPSE inventory. This is because BC emissions in ECLIPSE inventory has very small seasonal variation. Monthly BC emissions of India in ECLIPSE (excluding GFED) inventory vary from 93.7 Gg in September to maximum 104.2 Gg in July mainly due to seasonal variation of agricultural waste burning, which varies from 1.2 Gg to 10.5 Gg. Together with GFED, there is less than 4.1% monthly variation of total BC emissions in a year in India.

As mentioned before, simulations for the year 2009 were carried out without including the wet-deposition process. When including wet-deposition for the year 2009, the

underestimation may even be larger than that reported here. However, in Figure 7b and 7c, we show a comparison for the year 2011 without and with wet deposition, respectively. It can be seen that the wet-deposition has very little effect and hardly produces perceptible differences between Figures 7b and 7c. Overall, wet-deposition reduces modelled BC values by only 8% when using the ECLIPSE inventory. Seasonally, the wet-deposition is found to be reducing modelled BC values by 5% in winter, 6% in spring, 14% in summer and 15% in autumn. Such seasonal influence is expected as the maximum rain over Gadanki is received during summer and autumn (cf. Fig. 1). There were about 76 days in the year 2011, when wet-deposition reduced the BC concentrations by more than 15%. In summary, wet-deposition is not a major factor that causes underestimation of model BC values over Gadanki. This is a result of relative short rainy season over major parts of India and the short transport times during the rainy season for a major fraction of the BC between its emission and the arrival at Gadanki, rendering precipitation scavenging an ineffective process for this particular site. This result is site-specific and does not imply that wet deposition is globally of minor importance. On the contrary, it is the main removal mechanism for BC in the model.

In Figure 8, the average age spectra (measuring the time between BC emission and BC arrival at Gadanki) of modelled BC values estimated using the ECLIPSE inventory are shown for the full year as well as for the four seasons. One can see that on average about 30% to 40% of BC mass is of age 4 days or more. During winter this value increases to 65%. In other words, a large fraction of BC mass during winter is due to long-range transport of BC particles from Northern India. If the dry deposition process is the reason for underestimation then one may expect larger model biases in winter. Instead, during winter, the comparison between model and observations is better. Hence, dry deposition may also not be an important factor for causing the underestimation.

The differences between observation and model are in fact correlated to biomass burning activity (cf. Fig. 2; Also, see seasonal maps of fire hotspots overlaid on PES in supporting material). Since, SAFAR-India inventory considers only anthropogenic emissions and do not include forest-fire emissions, such underestimation during spring (open biomass burning season) is expected for it. The RETRO inventory has BC emissions from forest-fires and in case of ECLIPSE inventory, forest-fire emissions are included from GFEDv3. In-spite of this

ECLIPSE and RETRO inventories have similar underestimation like SAFAR-India during spring. The modelled BC values using ECLIPSE and RETRO are about a factor 2.1 and 3.5 lower than the observed BC concentration (2.8 $\mu g/m^3$) respectively. The variation of monthly BC emissions from forest-fires in GFED and RETRO are similar to the monthly variations of FRP shown in Fig. 2 with maximum emissions of 45 Gg in case of GFED and 24 Gg in case of RETRO during March. However, BC emissions from forest fires over India in GFED and RETRO are lower than anthropogenic emissions by a factor 23 annually and by a factor of 2.2 to 2.8 during March (peak biomass burning season). The year 2009 was a drought year and had a higher number of forest-fire events. This is reflected in higher observed BC concentrations during spring of 2009 compared to the spring of 2011 (cf. Fig. 4 and 7). In spite of the low BC values during spring of 2011 (being a normal year from drought or forest-fire events perspective), all the three inventories still significantly underestimate the observations (cf. Table 2). The fraction of BC particles of age less than 4 days is 61% in the year 2009 and 70% in the year 2011 (cf. Fig. 8). In other words, freshly emitted particles over Southern India form a major part of the total BC load during summer and spring (cf. Fig. 6). Hence, our analysis suggests that underestimation is due to underestimation of emissions over Southern India, however it is difficult to pin-point sectors that are being underestimated for BC emissions. Contextual information such as underestimation being correlated to FRP suggests that BC emissions from open-biomass-burning may be the main sector responsible for underestimation of BC concentration at Gadanki. Gustafsson et al. (2009) and Sheesley et al. (2012) apportioned carbonaceous aerosols using radiocarbon technique over two locations influenced by air-masses from India and found biomass burning contributing to the extent of 70% of total mass of carbonaceous aerosols. Pavuluri et al. (2011) studied correlation of black carbon with levoglucosan and non-sea-salt K^+ at Chennai (a major city in Southern India) and found that biomass burning is the major source of them during winter and summer. Lelieveld et al. (2001) estimated contribution of biomass burning in CO in range of 60% to 90% using correlation with CH_3CN and radiocarbon technique during Indian Ocean Experiment (INDOEX). However, underestimation of open biomass burning as source cannot explain fully the underestimation of BC concentration by the model during summer when biomass burning activity is low. A possibility exists that aethalometer may overestimate BC concentration during summer. Aethalometer relates absorption by particles on filter paper to

BC mass. During summer when wind speeds and direction are conducive for dust aerosol, atmosphere may have high level of dust amount. Dust is a weakly absorbing type of aerosol. Mass absorption cross-section of dust is 9 times lower than BC mass absorption cross-section (Zhang et al., 2008). However, during summer, when BC concentrations are low, absorption by dust particles can be significant part of total absorption by the particles on the filter paper and may be wrongly attributed to BC mass. In absence of chemical analysis, we rely on spectral signature of absorption coefficient for qualitative information on aerosol type. Zhang et al. (2008) have found inverse wavelength (λ^{-1}) dependence of the absorption coefficient for black carbon particles and no significant wavelength dependence for dust particles observed in China. Exponent of wavelength (in power-law form of relation between absorption coefficient and wavelength) is reported between -1.5 and -3 for BC particles emitted in biomass burning (Bergstrom et al., 2004; Kirchstetter et al., 2004; Bergstrom et al., 2007; Clarke et al., 2007). Spectral characteristics of dust particles vary from place to place and the wavelength exponent is reported between -2 and -3 for some of the places in Asia and Africa (Bergstrom et al., 2004; Fialho et al., 2005; Bergstrom et al., 2007). Monthly median values of wavelength exponent based on seven wavelengths of aethalometer at Gadanki are found to vary between -0.98 to -1.18 for year 2009 (Figure absorption_alpha_2009.png in supporting material). However, the variability as indicated by interquartile range is found to have increased significantly during summer, indicative of increase in heterogeneity of absorbing aerosol types during summer. Hence, dust aerosols may be a factor but it may not account for all the difference between model and observation during summer.

This suggests not only biomass burning but other anthropogenic emissions in South India are also underestimated. BC emission ratios vary within a country due to different stages of economic development (power plant and auto-mobile technology, environmental regulations enforcement). Changes, particularly environmental regulations and their implementation can be highly region/place specific. Moreover, the changes can be non-linear in time. Southern states in India are comparatively more industrialised than northern states but have lower population growth. If emission ratios are generalised for whole country or linear growth is assumed based on population, it may introduce errors in emission inventory. In addition, small scale anthropogenic biomass burning can be significant. While satellite based fire detection are low during summer, radiocarbon based and levoglucosan based BC apportionment suggest

significant contribution of BC from biomass burning during summer (Pavuluri et al., 2011; Sheesley et al., 2012). Indoor biomass burning and small scale agricultural waste burning will go unnoticed in satellite data due to increased cloudiness during summer. When overall BC concentrations are low, underestimation of these sources may cause significant fractional error in the estimated BC concentrations.

Overall, though underestimation of anthropogenic emissions cannot be ruled out, underestimation of BC concentration at Gadanki is likely related to underestimation of BC emission fluxes from forest fires and/or agricultural waste burning over Southern India, particularly during spring.

4.3.1 Case studies

Since, emission inventories for the years 2009 and 2011 are kept the same, the difference in model values between these two years is purely due to meteorology. In the rest of the article, we focus on the year 2009. As noted in the previous section, the model underestimates BC values during spring and summer. The underestimation of BC concentrations may be related to underestimation of biomass burning activity during the dry season and sub-regionally incorrect anthropogenic emission fluxes. Here we discuss a few cases from the year 2009 which provide insight into these aspects.

In Figure 9, a comparison of modelled and observed BC concentration over Gadanki for the year 2009 is shown. It is similar to Fig. 7(a), but zoomed-in for three different periods. Note the sudden decrease in BC concentration for both observation and model on 8th January in Fig. 9(a). From 1st January to 6th January, high PES extended along the east coast of India and Indo-Gangetic Basin (IGB) region. However, from 7th January onward PES region started shifting away from the coastline towards the central Bay of Bengal (BoB). On 8th January, high PES region was a narrow region stretching eastward up to Andaman Nicobar Island and then turned northward up to Bangladesh. Oceanic regions do not have many black carbon sources except for exhaust from ships plying in the region. Simultaneous decrease in observed and modelled values in this case is indicative of the fact that large part of BC observed over Gadanki is transported rather than of local origin. Notice that in the model, BC variations are mainly due to changes in air mass transport (and precipitation in case of year 2011) because the emissions are kept constant for at least one month. From 9th January onward, the high PES

region moves again closer to the east coast of India but does not penetrate deep into land. However, on 13th January, high PES region was found to be covering whole of Bangladesh, and Bihar and West Bengal states of India. On 13th January, a BC peak is found in observations and in the model. Again on 16th January, high PES region moved toward central BoB and away from East Coast of India (cf. Fig. 5b). However, unlike 8th January event, in this case, high PES region is a little further north and east in BoB and touches Southern Myanmar. The decrease in case of models is higher than it was found for 8th January but decrease in observed BC concentration is not as big as for 8th January. This is possible if emission fluxes over high PES region are underestimated.

From 16th January onward, PES region moves toward India systematically and deep in-land over IGB region. On 21st January PES region covers whole of West Bengal, Bihar and Delhi, and large parts of Orissa, Uttarpradesh and Haryana states of India in and around IGB. On 21st January both model and observation have high concentration close to 4 microgram and there are relatively small differences between model and observations. This is indicative that the inventory values are realistic for this region, although perhaps still underestimate true emissions.

During February to middle of March, observed BC concentrations are increasing whereas model values are systematically decreasing. During this period high PES region has moved away from India towards BoB, whereas PES region in immediate vicinity of Gadanki has moved southward over Tamil Nadu state of India. Large divergence between observation and model is an indication that the inventoried emission fluxes are significantly underestimated over Southern India. This is also a period of high biomass burning activity in the region of the high PES (cf. Fig. 2). Hence, under-estimation may be related specifically to under-estimation of open biomass burning in southern India.

From 22nd April, the high PES region has moved to the west of the observation site, over Karnataka state of India and the Arabian Sea (cf. Fig. 5d) and occasionally moving south of the observation site over entire Tamil Nadu. During later part of May, and June and July months, the high PES region is mostly over the Arabian Sea with very small region over land due to strong winds (cf. Fig 5c). Both model and observations have low values during this

period, however the model systematically underestimates the observations by factor of 2 to 3 (cf. Fig. 9b).

From 5th September onward PES region covers Andhra Pradesh, Madhya Pradesh and Gujarat states of India. On 22nd September, the model significantly over estimates the observation and for some days it remains higher than observations (cf. Fig. 9c). High PES region during this period lay over Andhra Pradesh and Tamil Nadu border and over southern Karnataka. From 16th October onward PES pattern moves entirely north of the observation site. In beginning the pattern covers Central and Western India but on 1st November, the PES pattern is similar to that found during January-February and extends all the way up to North West border of India covering the entire Indo-Gangetic region (cf. Fig. 5a). On this day, the concentration is the highest in model with similar values in observations. During September to December, differences between observation and model estimates are small.

Summarising the above description, observed and modelled BC values are high when winds are from Northern and Western India, with relatively small differences between model and observations, indicative of relatively small errors in the emission inventories over this region. When winds are from South or South Central India, the observed values are high but the model values are substantially lower. Coincidently this is also the period of high biomass burning activity over Southern India. The differences between the model and observation thus suggest that open biomass burning emissions over Southern India have been underestimated in all the three inventories.

5 Conclusions

Several field studies over India and in adjoining oceans have found high amount of absorbing aerosols. However, models are found to under-predict the observed high concentrations of absorbing aerosols. Using the Lagrangian particle dispersion model FLEXPART and three emission inventories, we compared the simulated BC concentrations with BC measurements at a rural site in southern India. As for the other models, FLEXPART underestimates the observed BC concentrations. We found that 93% to 95% of the model BC concentration is the result of emissions from India. Northern India is a major source of anthropogenic BC particles, but Southern India also has significant BC emissions. This study identifies potentially significant underestimate of emissions in Southern India, which is reflected in a

large difference in the observed and modelled BC values in Gadanki during spring when the winds are predominantly from the south. We suggest that the key source for which the emission fluxes may be underestimated is open biomass burning. This is not to rule out possibility that anthropogenic emissions may also be underestimated.

In the three emission inventories that we evaluated, ECLIPSE inventory has the highest emissions (1.2 Tg/yr), with similar emissions in the SAFAR-India inventory (1.1 Tg/yr). It is also reflected in the comparison between the modelled and observed BC concentration over Gadanki. Modelled BC values based on ECLIPSE and SAFAR-India are higher than the values based on the RETRO inventory. However, they are not high enough to resolve underestimation in most of the seasons. Overall ratio of observation to model is found to be 1.5 for SAFAR inventory, 1.7 for ECLIPSE inventory and 2.4 for RETRO inventory. Though ECLIPSE inventory has the highest emissions over India, it is SAFAR-India inventory that has the lowest ratio because of differences in spatial distribution in emission fluxes. SAFAR-India inventory has higher emission fluxes over Southern India compared to ECLIPSE.

Acknowledgements

Authors acknowledge the developers of the FLEXPART model and related software for visualisation and for providing the source code, which was obtained from http://flexpart.eu/ web-site. Authors also acknowledge National Center for Environmental Prediction/National Weather Service/NOAA/US Department of Commerce (2000) for providing GFS-FNL analysis data. Authors acknowledge developers of BC emission inventories namely (1) SAFAR-India inventory made available through Emissions of atmospheric Compounds & Compilation of Ancillary Data (ECCAD) – the GEIA database project from the web-site http://eccad.sedoo.fr/, (2) ECLIPSE (Evaluating the Climate and Air Quality Impacts of Short-Lived Pollutants; Project no. 282688) made available from the web-site http://eclipse.nilu.no/ and (3) RETRO (REanalysis of the TROpospheric chemical composition over the past 40 years) made available from the web-site http://retro.enes.org/. Authors acknowledge the use of FIRMS data from LANCE (the Land Atmosphere Near-real time Capability for EOS) system operated by ESDIS (the NASA/GSFC/Earth Science Data and Information System) with funding provided by NASA/HQ. Authors acknowledge the use of rainfall estimates obtained from TRMM satellite through GIOVANNI online data system,

developed and maintained by the NASA GES DISC to provide rainfall maps in supporting material. Authors acknowledge T. N. Rao and his team members for providing weather station data. KR and HG thank Sabine Eckhardt and Rona Thompson for helping in running of the FLEXPART model. KR thanks European Science Foundation (ESF) Research Network TTORCH for supporting her participation in FLEXPART training course. Authors thank Department of Space, Government of India for funding the climate observatory operational at NARL, Gadanki. A. Stohl and Z. Klimont were supported by the European Union Seventh Framework Programme (FP7/2007-2013) under grant agreement no 282688 – ECLIPSE.

References

Ackerman, A. S., Toon, O. B., Stevens, D. E., Heymsfield, A. J., Ramanathan, V. and Welton, E. J.: Reduction of Tropical Cloudiness by Soot, Science, 288, 1042-1047, doi:10.1126/science.288.5468.1042, 2000.

Amann, M., Bertok, I., Borken-Kleefeld, J., Cofala, J., Heyes, C., Höglund-Isaksson, L., Klimont, Z., Nguyen, B., Posch, M., Rafaj, P., Sandler, R., Schöpp, W., Wagner, F. and Winiwarter, W.: Cost-effective control of air quality and greenhouse gases in Europe: Modeling and policy applications, Environmental Modelling & Software, 26, 1489-1501, doi:10.1016/j.envsoft.2011.07.012, 2011.

Beegum, S., Moorthy, K. K., Babu, S., Satheesh, S., Vinoj, V., Badarinath, K., Safai, P., Devara, P., Singh, S., Vinod, Dumka, U. C. and Pant, P.: Spatial distribution of aerosol black carbon over India during pre-monsoon season, Atmos. Environ., 43, 1071-1078, doi:10.1016/j.atmosenv.2008.11.042, 2009.

Bergstrom, R. W., Pilewskie, P., Pommier, J., Rabbette, M., Russell, P. B., Schmid, B., Redemann, J., Higurashi, A., Nakajima, T. and Quinn, P. K.: Spectral absorption of solar radiation by aerosols during ACE-Asia, J. Geophys. Res.-Atmos., 109, D19S15+, doi:http://dx.doi.org/10.1029/2003JD004467, 2004.

Bergstrom, R. W., Pilewskie, P., Russell, P. B., Redemann, J., Bond, T. C., Quinn, P. K. and Sierau, B.: Spectral absorption properties of atmospheric aerosols, Atmos. Chem. Phys., 7, 5937-5943, 2007.

Bond, T. C., Doherty, S. J., Fahey, D. W., Forster, P. M., Berntsen, T., DeAngelo, B. J., Flanner, M. G., Ghan, S., Kärcher, B., Koch, D., Kinne, S., Kondo, Y., Quinn, P. K., Sarofim, M. C., Schultz, M. G., Schulz, M., Venkataraman, C., Zhang, H., Zhang, S., Bellouin, N., Guttikunda, S. K., Hopke, P. K., Jacobson, M. Z., Kaiser, J. W., Klimont, Z., Lohmann, U., Schwarz, J. P., Shindell, D., Storelvmo, T., Warren, S. G. and Zender, C. S.: Bounding the role of black carbon in the climate system: A scientific assessment, J. Geophys. Res., 118, 5380-5552, doi:10.1002/jgrd.50171, 2013.

Bond, T. C., Streets, D. G., Yarber, K. F., Nelson, S. M., Woo, J.-H. and Klimont, Z.: A technology-based global inventory of black and organic carbon emissions from combustion, J. Geophys. Res.-Atmos., 109, D14203+, doi:10.1029/2003JD003697, 2004.

Clarke, A., Mcnaughton, C., Kapustin, V., Shinozuka, Y., Howell, S., Dibb, J., Zhou, J., Anderson, B., Brekhovskikh, V., Turner, H. and Pinkerton, M.: Biomass burning and pollution aerosol over North America: Organic components and their influence on spectral optical properties and humidification response, J. Geophys. Res.-Atmos., 112, D12S18+, doi:http://dx.doi.org/10.1029/2006JD007777, 2007.

Cooke, W. F., Liousse, C., Cachier, H. and Feichter, J.: Construction of a 1° × 1° fossil fuel emission data set for carbonaceous aerosol and implementation and radiative impact in the ECHAM4 model, J. Geophys. Res., 104, 22137-22162, doi:10.1029/1999jd900187, 1999.

Davies, D. K., Ilavajhala, S., Wong, M. M. and Justice, C. O.: Fire Information for Resource Management System: Archiving and Distributing MODIS Active Fire Data, Geoscience and Remote Sensing, IEEE Transactions on, 47, 72-79, doi:10.1109/tgrs.2008.2002076, 2009.

Dickerson, R. R., Andreae, M. O., Campos, T., Mayol-Bracero, O. L., Neususess, C. and Streets, D. G.: Analysis of black carbon and carbon monoxide observed over the Indian Ocean: Implications for emissions and photochemistry, J. Geophys. Res., 107, 8017, doi:10.1029/2001JD000501, 2002.

Fialho, P., Hansen, A. and Honrath, R.: Absorption coefficients by aerosols in remote areas: a new approach to decouple dust and black carbon absorption coefficients using seven-wavelength Aethalometer data, J. Aerosol Sci., 36, 267-282, doi:10.1016/j.jaerosci.2004.09.004, 2005.

Gadhavi, H. and Jayaraman, A.: Absorbing aerosols: contribution of biomass burning and implications for radiative forcing, Ann. Geophys., 28, 103-111, doi:10.5194/angeo-28-103-2010, 2010.

Ganguly, D., Ginoux, P., Ramaswamy, V., Winker, D. M., Holben, B. N. and Tripathi, S. N.: Retrieving the composition and concentration of aerosols over the Indo-Gangetic basin using CALIOP and AERONET data, Geophys. Res. Lett., 36, L13806+, doi:10.1029/2009GL038315, 2009.

Ganguly, D., Jayaraman, A. and Gadhavi, H.: Physical and optical properties of aerosols over an urban location in western India: Seasonal variabilities, J. Geophys. Res., 111, D24206+, doi:10.1029/2006JD007392, 2006a.

Ganguly, D., Jayaraman, A., Gadhavi, H. and Rajesh, T. A.: Features in wavelength dependence of aerosol absorption observed over central India, Geophys. Res. Lett., 32, L13821+, doi:10.1029/2005GL023023, 2005.

Ganguly, D., Jayaraman, A., Rajesh, T. A. and Gadhavi, H.: Wintertime aerosol properties during foggy and nonfoggy days over urban center Delhi and their implications for shortwave radiative forcing, J. Geophys. Res., 111, D15217+, doi:10.1029/2005JD007029, 2006b.

Giglio, L., Descloitres, J., Justice, C. O. and Kaufman, Y. J.: An Enhanced Contextual Fire Detection Algorithm for MODIS, Remote Sens. Environ., 87, 273-282, doi:10.1016/s0034-4257(03)00184-6, 2003.

Gustafsson, O., Krusa, M., Zencak, Z., Sheesley, R. J., Granat, L., Engstrom, E., Praveen, P. S., Rao, P. S. P., Leck, C. and Rodhe, H.: Brown Clouds over South Asia: Biomass or Fossil Fuel Combustion?, Science, 323, 495-498, doi:http://dx.doi.org/10.1126/science.1164857, 2009.

Hansen, A. D. A.: The Aethalometer, Berkeley, California,USA, available at: http://www.mageesci.com/images/stories/docs/Aethalometer_book_2005.07.03.pdf (last access: 13 January 2015), 2005.

Haywood, J. M. and Ramaswamy, V.: Global sensitivity studies of the direct radiative forcing due to anthropogenic sulfate and black carbon aerosols, J. Geophys. Res., 103, 6043-6058, doi:10.1029/97JD03426, 1998.

Hertel, O., Christensen, J., Runge, E. H., Asman, W. A. H., Berkowicz, R., Hovmand, M. F. and Hov, O.: Development and testing of a new variable scale air pollution model -- ACDEP, Atmos. Environ., 29, 1267-1290, 1995.

Jacobson, M. Z.: Strong radiative heating due to the mixing state of black carbon in atmospheric aerosols, Nature, 409, 695-697, doi:10.1038/35055518, 2001.

Jayaraman, A., Gadhavi, H., Ganguly, D., Misra, A., Ramachandran, S. and Rajesh, T. A.: Spatial variations in aerosol characteristics and regional radiative forcing over India: Measurements and modeling of 2004 road campaign experiment, Atmos. Environ., 40, 6504-6515, doi:10.1016/j.atmosenv.2006.01.034, 2006.

Joseph, S., Anitha, K. and Murthy, M. S. R.: Forest fire in India: a review of the knowledge base, Journal of Forest Research, 14, 127-134, doi:10.1007/s10310-009-0116-x, 2009.

Justice, C., Giglio, L., Boschetti, L., Roy, D., Csiszar, I., Morisette, J. and Kaufman, Y.: Algorithm Technical Background Document MODIS FIRE PRODUCTS, NASA, 2006.

Kirchstetter, T. W., Novakov, T. and Hobbs, P. V.: Evidence that the spectral dependence of light absorption by aerosols is affected by organic carbon, J. Geophys. Res.-Atmos., 109, D21208+, doi:http://dx.doi.org/10.1029/2004JD004999, 2004.

Klimont, Z., Cofala, J., Xing, J., Wei, W., Zhang, C., Wang, S., Kejun, J., Bhandari, P., Mathur, R., Purohit, P., Rafaj, P., Chambers, A., Amann, M. and Hao, J.: Projections of SO 2 , NO x and carbonaceous aerosols emissions in Asia, Tellus B, 61, 602-617, doi:10.1111/j.1600-0889.2009.00428.x, 2009.

Klimont, Z., Hoglund, L., Heyes, C., Rafaj, P., Schoepp, W., Cofala, J., Borken-Kleefeld, J., Purohit, P., Kupiainen, K., Winiwarter, W., Amann, M., Zhao, B., Wang, S. X., Bertok, I. and Sander, R.: Global scenarios of air pollutants and methane: 1990-2050, in preparation for ACPD, 2015a.

Klimont, Z., Kupiainen, K., Heyes, C., Cofala, J., Rafaj, P., Höglund-Isaksson, L., Borken, J., Schöpp, W., Winiwarter, W., Purohit, P., Bertok, I. and Sander, R.: ECLIPSE V4a: Global emission data set developed with the GAINS model for the period 2005 to 2050: key features and principal data sources, International Institute for Applied Systems Analysis (IIASA), Schlossplatz 1, 2361 Laxenburg, Austria, 8 pp., available at:

http://eccad.sedoo.fr/eccad_extract_interface/JSF/page_login.jsf (last access: 13 January 2015), 2013.

Klimont, Z., Kupiainen, K., Heyes, C., Purohit, P., Cofala, J., Rafaj, P., Borken-Kleefeld, J. and Schoepp, W.: Global anthropogenic emissions of particulate matter, In preparation, 2015b.

Kupiainen, K. and Klimont, Z.: Primary emissions of fine carbonaceous particles in Europe, Atmos. Environ., 41, 2156-2170, doi:10.1016/j.atmosenv.2006.10.066, 2007.

Lelieveld, J., Crutzen, P. J., Ramanathan, V., Andreae, M. O., Brenninkmeijer, C. A. M., Campos, T., Cass, G. R., Dickerson, R. R., Fischer, H., de Gouw, J. A., Hansel, A., Jefferson, A., Kley, D., de Laat, A. T. J., Lal, S., Lawrence, M. G., Lobert, J. M., Mayol-Bracero, O. L., Mitra, A. P., Novakov, T., Oltmans, S. J., Prather, K. A., Reiner, T., Rodhe, H., Scheeren, H. A., Sikka, D. and Williams, J.: The Indian Ocean Experiment: Widespread Air Pollution from South and Southeast Asia, Science, 291, 1031-1036, doi:10.1126/science.1057103, 2001.

McMahon, T. A. and Denison, P. J.: Empirical atmospheric deposition parameters—A survey, Atmospheric Environment, 13, 571-585, doi:10.1016/0004-6981(79)90186-0, 1979.

Moorthy, K. K., Beegum, S. N., Srivastava, N., Satheesh, S., Chin, M., Blond, N., Babu, S. S. and Singh, S.: Performance evaluation of chemistry transport models over India, Atmos. Environ., 71, 210-225, doi:10.1016/j.atmosenv.2013.01.056, 2013.

Nair, V. S., Solmon, F., Giorgi, F., Mariotti, L., Babu, S. S. S. and Moorthy, K. K.: Simulation of south asian aerosols for regional climate studies, J. Geophys. Res., 117, 1-17, doi:10.1029/2011JD016711, 2012.

National Center for Environmental Prediction/National Weather Service/NOAA/U.S. Department of Commerce: NCEP FNL Operational Model Global Tropospheric Analyses continuing from July 1999, , Research Data Archive at the National Center for Atmospheric Research, 2000.

Pavuluri, C. M., Kawamura, K., Aggarwal, S. G. and Swaminathan, T.: Characteristics, seasonality and sources of carbonaceous and ionic components in the tropical aerosols from Indian region, Atmos. Chem. Phys., 11, 8215-8230, doi:10.5194/acp-11-8215-2011, 2011.

Raghavendra Kumar, K., Narasimhulu, K., Balakrishnaiah, G., Reddy, B. S. K., Gopal, K. R., Reddy, R. R., Satheesh, S. K., Moorthy, K. K. and Babu, S. S.: Characterization of aerosol black carbon over a tropical semi-arid region of Anantapur, India, Atmos. Res., 100, 12-27, doi:10.1016/j.atmosres.2010.12.009, 2011.

Ramachandran, S. and Kedia, S.: Black carbon aerosols over an urban region: Radiative forcing and climate impact, J. Geophys. Res., 115, D10202+, doi:10.1029/2009JD013560, 2010.

Ramachandran, S. and Rajesh, T. A.: Black carbon aerosol mass concentrations over Ahmedabad, an urban location in western India: Comparison with urban sites in Asia, Europe, Canada, and the United States, J. Geophys. Res., 112, D06211+, doi:10.1029/2006JD007488, 2007.

Sahu, S. K., Beig, G. and Sharma, C.: Decadal growth of black carbon emissions in India, Geophys. Res. Lett., 35, L02807+, doi:10.1029/2007GL032333, 2008.

Schultz, M., Backman, L., Balkanski, Y., Bjoerndalsaeter, S., Brand, R., Burrows, J., Dalsoeren, S., de Vasconcelos, M., Grodtmann, B., Hauglustaine, D., Heil, A., Hoelzemann, J., Isaksen, I., Kaurola, J., Knorr, W., Ladstaetter-Weißenmayer, A., Mota, B., Oom, D., Pacyna, J., Panasiuk, D., Pereira, J., Pulles, T., Pyle, J., Rast, S., Richter, A., Savage, N., Schnadt, C., Schulz, M., Spessa, A., Staehelin, J., Sundet, J., Szopa, S., Thonicke, K., van het Bolscher, M., van Noije, T., van Velthoven, P. and A.F. Vik, F. W.: REanalysis of the TROpospheric chemical composition over the past 40 years (RETRO) — A long-term global modeling study of tropospheric chemistry: Final Report, Max Planck Institute for Meteorology, Hamburg, Julich/Hamburg, Germany, 126 pp, 2007.

Schultz, M. and Rast, S.: Emission data sets and methodologies for estimating emissions, Max Planck Institute for Meteorology, Hamburg, Hamburg, Germany, 77 pp, 2007.

Schultz, M. G., Heil, A., Hoelzemann, J. J., Spessa, A., Thonicke, K., Goldammer, J. G., Held, A. C., Pereira, J. M. C. and van het Bolscher, M.: Global wildland fire emissions from 1960 to 2000, Global Biogeochem. Cycles, 22, GB2002+, doi:10.1029/2007gb003031, 2008.

Seibert, P. and Frank, A.: Source-receptor matrix calculation with a Lagrangian particle dispersion model in backward mode, Atmos. Chem. Phys., 4, 51-63, 2004.

Sheesley, R. J., Kirillova, E., Andersson, A., Krusa, M., Praveen, P. S., Budhavant, K., Safai, P. D., Rao, P. S. P. and Gustafsson, Ö.: Year-round radiocarbon-based source apportionment of carbonaceous aerosols at two background sites in South Asia, J. Geophys. Res., 117, D10202+, doi:10.1029/2011jd017161, 2012.

Stohl, A., Forster, C., Frank, A., Seibert, P. and Wotawa, G.: Technical note: The Lagrangian particle dispersion model FLEXPART version 6.2, Atmos. Chem. Phys., 5, 2461-2474, doi:10.5194/acp-5-2461-2005, 2005.

Stohl, A., Hittenberger, M. and Wotawa, G.: Validation of the lagrangian particle dispersion model FLEXPART against large-scale tracer experiment data, Atmos. Environ., 32, 4245-4264, doi:10.1016/s1352-2310(98)00184-8, 1998.

Stohl, A., Klimont, Z., Eckhardt, S., Kupiainen, K., Shevchenko, V. P., Kopeikin, V. M. and Novigatsky, A. N.: Black carbon in the Arctic: the underestimated role of gas flaring and residential combustion emissions, Atmos. Chem. Phys., 13, 8833-8855, doi:10.5194/acp-13-8833-2013, 2013.

Suresh Babu, S. and Moorthy, K. K.: Aerosol black carbon over a tropical coastal station in India, Geophys. Res. Lett., 29, 2098+, doi:10.1029/2002GL015662, 2002.

Suresh Babu, S., Satheesh, S. K. and Moorthy, K. K.: Aerosol radiative forcing due to enhanced black carbon at an urban site in India, Geophys. Res. Lett., 29, 1880+, doi:10.1029/2002GL015826, 2002.

Venkataraman, C., Habib, G., Eiguren-Fernandez, A., Miguel, A. H. and Friedlander, S. K.: Residential Biofuels in South Asia: Carbonaceous Aerosol Emissions and Climate Impacts, Science, 307, 1454-1456, doi:10.1126/science.1104359, 2005.

Vinoj, V., Satheesh, S. K. and Moorthy, K. K.: Optical, radiative, and source characteristics of aerosols at Minicoy, a remote island in the southern Arabian Sea, J. Geophys. Res., 115, D01201+, doi:10.1029/2009JD011810, 2010.

van der Werf, G. R., Randerson, J. T., Giglio, L., Collatz, G. J., Mu, M., Kasibhatla, P. S., Morton, D. C., DeFries, R. S., Jin, Y. and van Leeuwen, T. T.: Global fire emissions and the contribution of deforestation, savanna, forest, agricultural, and peat fires (1997–2009), Atmos. Chem. Phys., 10, 11707-11735, doi:10.5194/acp-10-11707-2010, 2010.

1 Yasa, Z., Amer, N. M., Rosen, H., Hansen, A. D. A. and Novakov, T.: Photoacoustic
2 investigation of urban aerosol particles, Appl. Opt., 18, 2528-2530,
3 doi:10.1364/AO.18.002528, 1979.

4 Zhang, X. Y., Wang, Y. Q., Zhang, X. C., Guo, W., Niu, T., Gong, S. L., Yin, Y., Zhao, P., Jin,
5 J. L. and Yu, M.: Aerosol monitoring at multiple locations in China: contributions of EC and
6 dust to aerosol light absorption, Tellus B, 60, 647-656, doi:10.1111/j.1600-
7 0889.2008.00359.x, 2008.

Table 1: FLEXPART model set-up for retroplume runs from Gadanki

Input Meteorological data	NCEP-GFS data at 1° x 1° global
Tracer	Black Carbon aerosol
Point of origin for retroplume	Gadanki (13.48° N, 79.18° E, 365 m above mean sea level), altitude: 0 – 100 meter.
Output grid	Horizontal: 1° X 1° global; Vertical: 0-100, 100-3000, 3000-5000 meters above ground.
Mode	Backward runs
Number of days backward for each release	10 days
Dry Deposition	Enabled for 2009 and 2011
Convection	Enabled for 2009 and 2011
Wet deposition	Enabled only for year 2011
Dry deposition parameters	Density (rho) = 1400 kg/m^3 Mean Diameter (d_p) = 0.25 µm Sigma of log-normal distribution (dsig) = 1.25
Below-cloud scavenging parameters	Scavenging coefficient at rain fall rate 1mm/hr (A) = $2x10^{-7}$ s^{-1} Dependency factor (B) = 0.62

Table 2: Average, ratio, bias, RMSD and correlation coefficient between modelled and observed BC concentrations when using different inventories for the years 2009 and 2011.

		2009*				**2011***			
		Obs.	**SAFAR**	**ECLIPSE**	**RETRO**	**Obs.**	**SAFAR**	**ECLIPSE**	**RETRO**
Mean (µg/m^3)	**All**	2.308	1.494	1.378	0.936	2.279	1.483	1.454	1.05
	Winter	3.405	2.179	2.182	1.643	3.213	2.367	2.624	2.103
	Spring	2.998	1.452	1.366	0.835	2.591	1.345	1.242	0.800
	Summer	1.181	0.595	0.496	0.232	1.234	0.595	0.467	0.229
	Autumn	1.700	1.805	1.525	1.087	2.110	1.653	1.518	1.118
Ratio (Obs/Model)	**All**	1	1.545	1.675	2.465	1	1.537	1.568	2.162
	Winter	1	1.563	1.561	2.072	1	1.357	1.225	1.528
	Spring	1	2.065	2.196	3.593	1	1.926	2.086	3.239

	Summer	1	1.986	2.38	5.098	1	2.075	2.641	5.396
	Autumn	1	0.942	1.115	1.564	1	1.277	1.390	1.888
Bias (µg/m^3) (Model-Obs)	**All**	---	-0.814	-0.930	-1.372	---	-0.796	-0.825	-1.225
	Winter	---	-1.226	-1.224	-1.762	---	-0.846	-0.589	-1.110
	Spring	---	-1.547	-1.633	-2.164	---	-1.246	-1.349	-1.791
	Summer	---	-0.586	-0.684	-0.949	---	-0.639	-0.767	-1.006
	Autumn	---	0.104	-0.175	-0.613	---	-0.458	-0.592	-0.992
RMSD (µg/m^3)	**All**	---	1.401	1.419	1.726	---	1.082	1.254	1.448
	Winter	---	1.637	1.691	2.006	---	1.216	1.536	1.498
	Spring	---	2.017	2.031	2.457	---	1.426	1.495	1.917
	Summer	---	0.669	0.752	0.992	---	0.709	0.826	1.053
	Autumn	---	0.809	0.710	0.936	---	0.821	1.015	1.163
Correlation Coefficient (R)	**All**	---	0.483	0.542	0.543	---	0.726	0.661	0.690
	Winter	---	0.138	0.036	0.021	---	0.473	0.334	0.375
	Spring	---	0.063	0.249	0.422	---	0.501	0.605	0.560
	Summer	---	0.483	0.439	0.431	---	0.587	0.545	0.561
	Autumn	---	0.616	0.646	0.547	---	0.738	0.709	0.729

Winter - December to February
Spring – March to May
Summer – June to August
Autumn – September to November
RMSD – Root mean square deviation
*Note:
1 Calculations for 2011 are with wet deposition
2 Calculations for 2009 are without wet deposition
3 ECLIPSE inventory includes ECLIPSE v5, GFED v3 and Shipping emissions

1

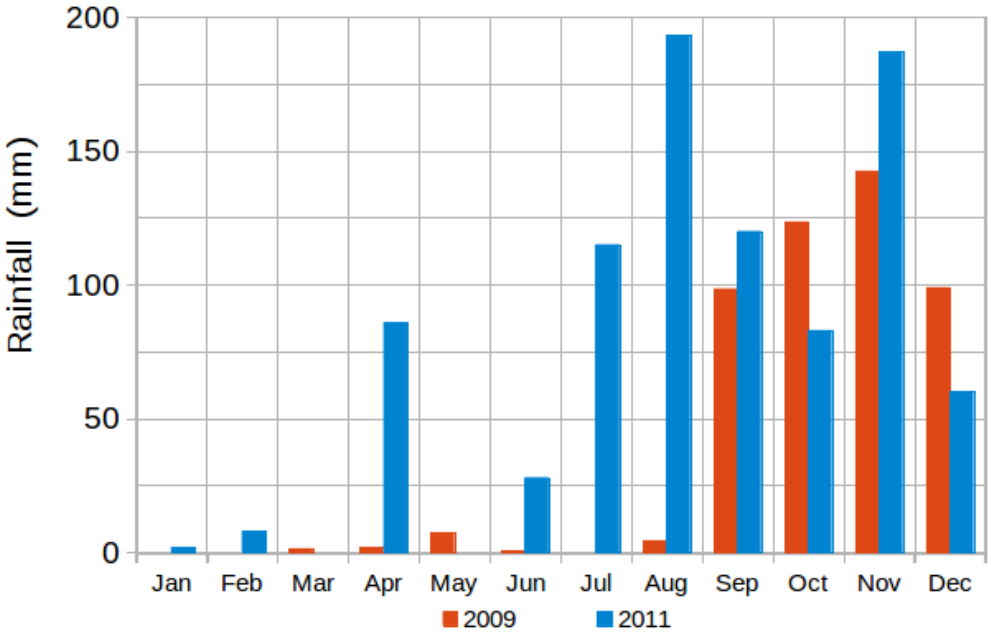

Figure 1: Monthly precipitation amounts over Gadanki during 2009 and 2011.

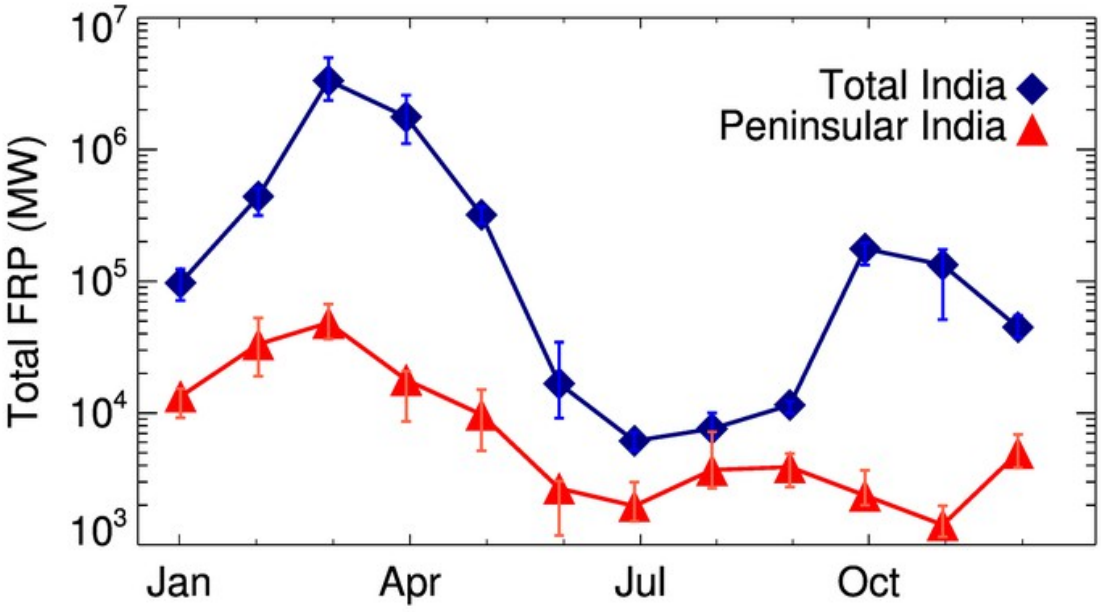

Figure 2: Monthly median fire radiative power values obtained from MODIS satellite for whole India and peninsular India (south of 18° N latitude).

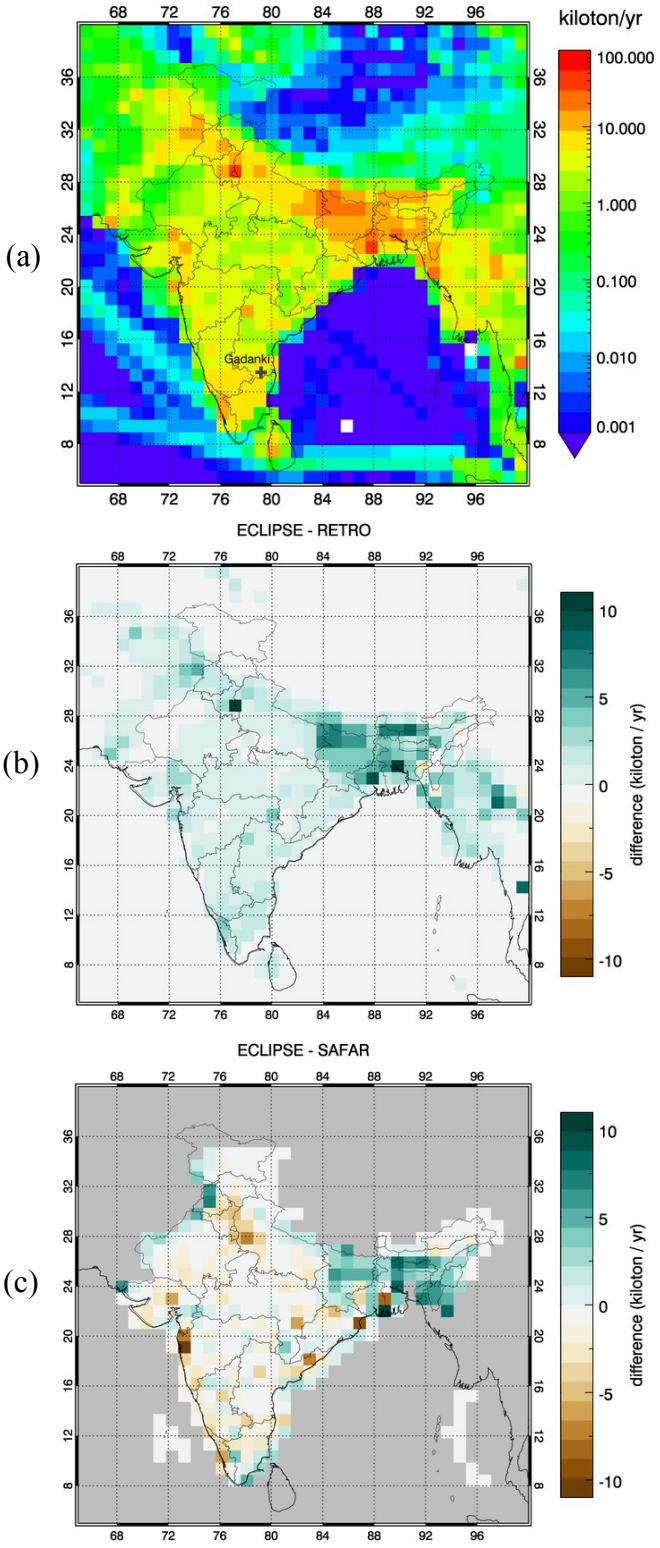

Figure 3: (a) ECLIPSE (ECLIPSE v5 + GFED v3) black carbon emission inventory over South Asia. (b) Difference between the ECLIPSE and RETRO emissions (ECLIPSE – RETRO). (c) difference between ECLIPSE and SAFAR India emissions (ECLIPSE –

SAFAR). Here and in rest of the article political borders are shown for cursory region identification and may not be accurate.

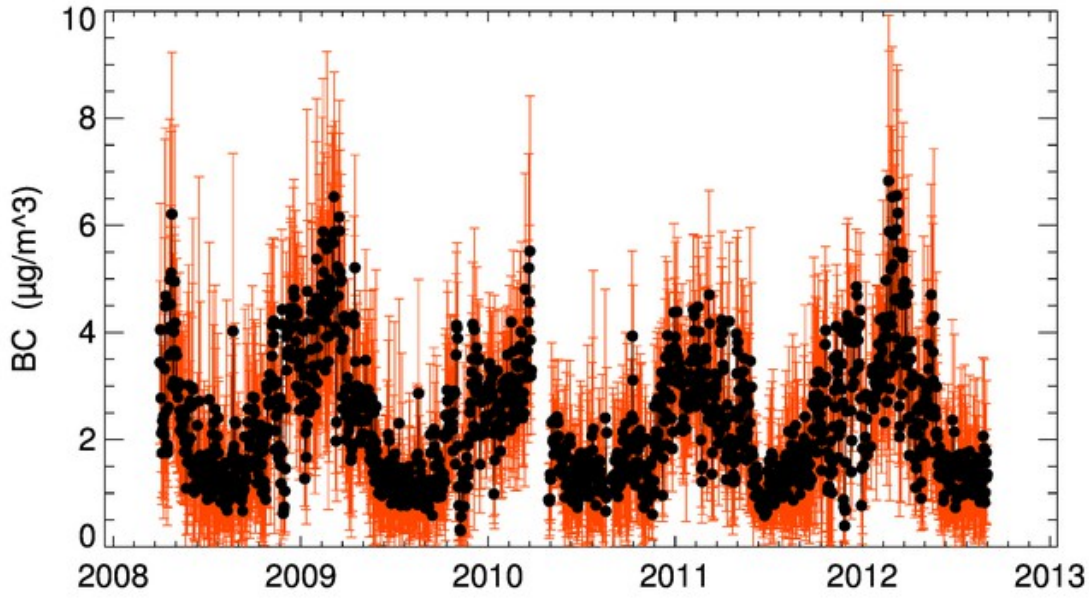

Figure 4: Daily mean black carbon concentration observed at Gadanki (black dots) and their ±1σ standard deviation (orange vertical bars).

1

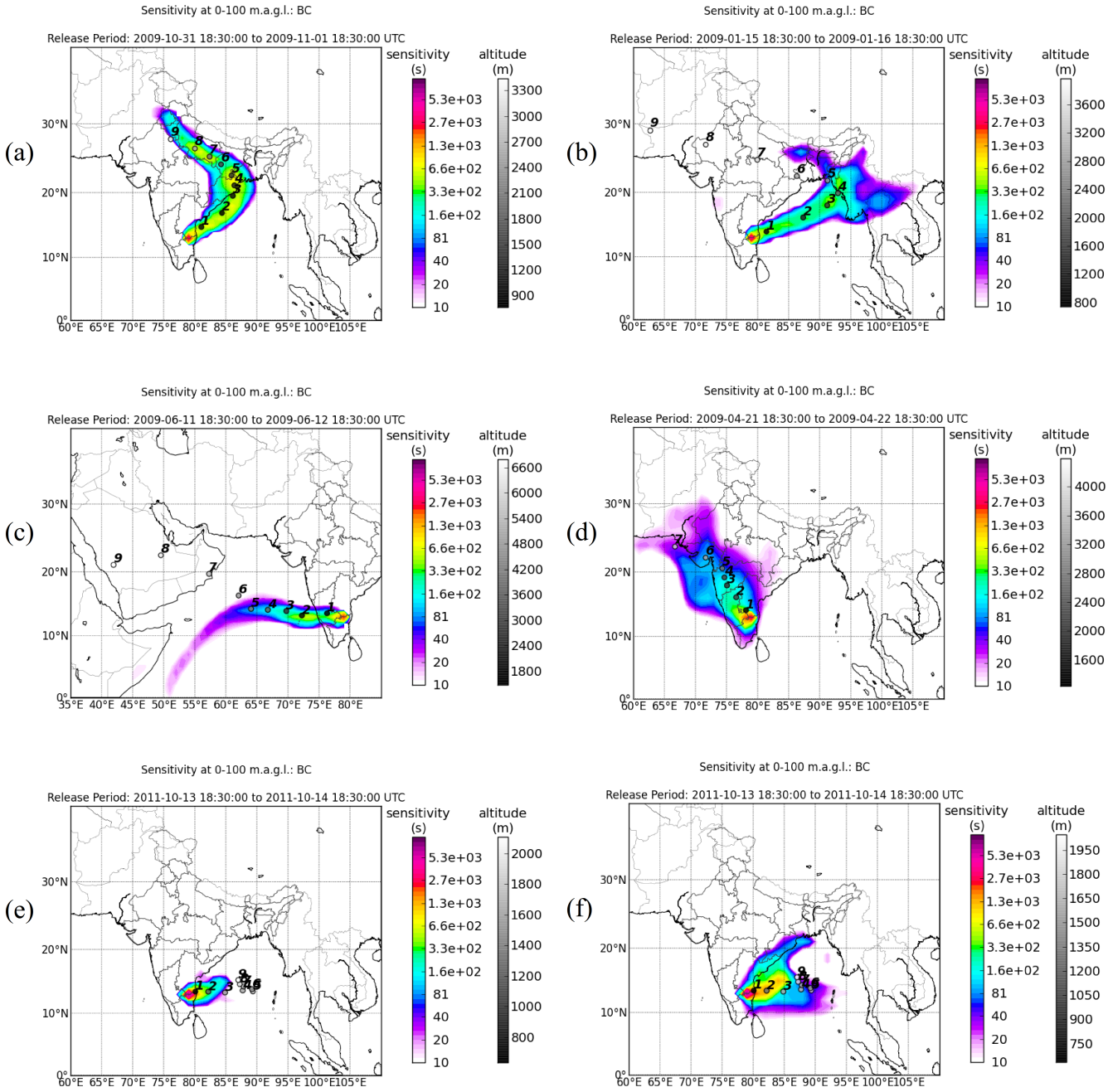

2 Figure 5: Selected examples of footprint potential emission sensitivity (PES) maps (also
3 known as source-receptor relationships) using 10 days of backward runs (retroplumes) of
4 FLEXPART from Gadanki. Figures (e) and (f) are PES maps of 14 Oct 2011 local time with
5 and without wet-deposition respectively. See supporting material for the PES maps for other
6 days.

(a)

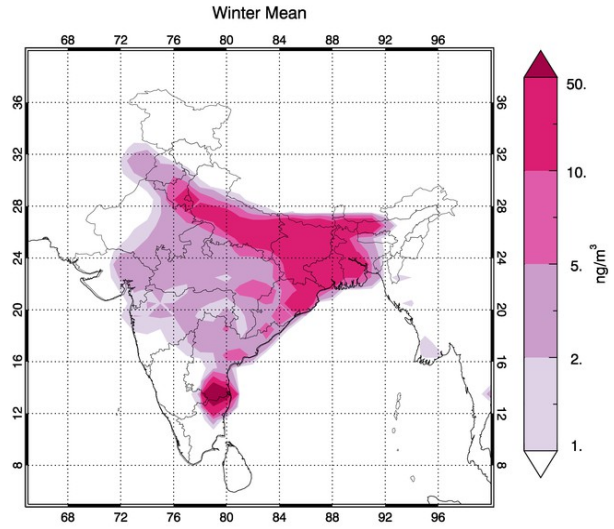
Winter Mean
68 72 76 80 84 88 92 96
36 32 28 24 20 16 12 8
50.
10.
5.
2.
1.
ng/m3

(b)

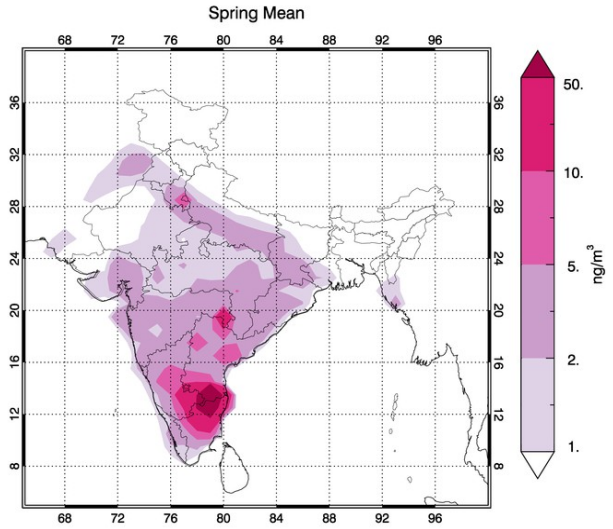
Spring Mean
68 72 76 80 84 88 92 96
36 32 28 24 20 16 12 8
50.
10.
5.
2.
1.
ng/m3

(c)

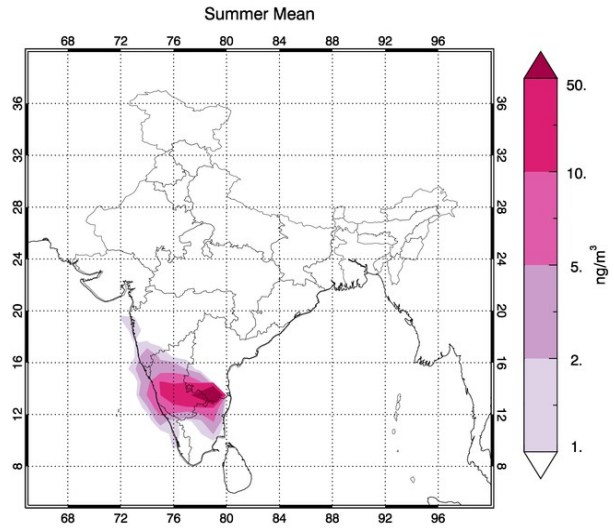
Summer Mean
68 72 76 80 84 88 92 96
36 32 28 24 20 16 12 8
50.
10.
5.
2.
1.
ng/m3

(d)

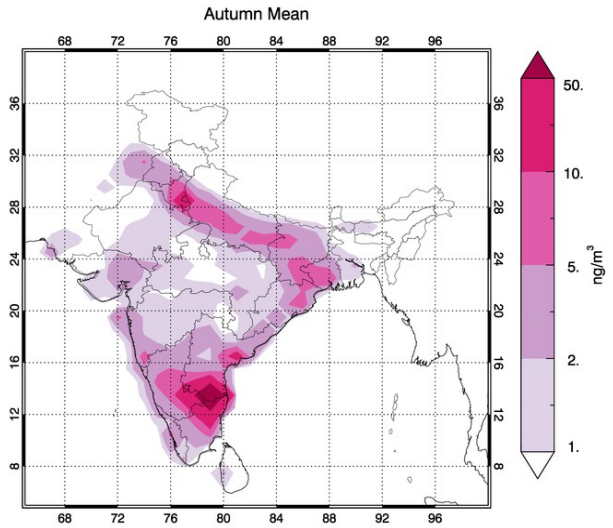
Autumn Mean
68 72 76 80 84 88 92 96
36 32 28 24 20 16 12 8
50.
10.
5.
2.
1.
ng/m3

(e)

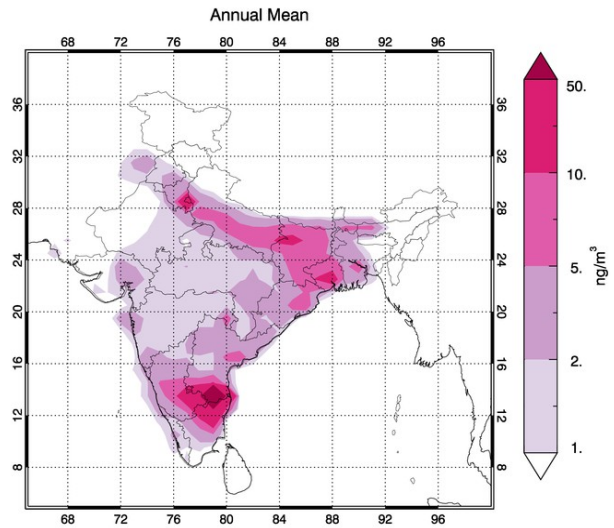
Annual Mean
68 72 76 80 84 88 92 96
36 32 28 24 20 16 12 8
50.
10.
5.
2.
1.
ng/m3

Figure 6: Black carbon source contribution (per 1°x1° grid-cell) maps based on FLEXPART retroplume calculations and the ECLIPSE inventory. Values are for seasonal averages i.e. (a) winter, (b) spring, (c) summer, (d) autumn, and (e) annual average for year 2009.

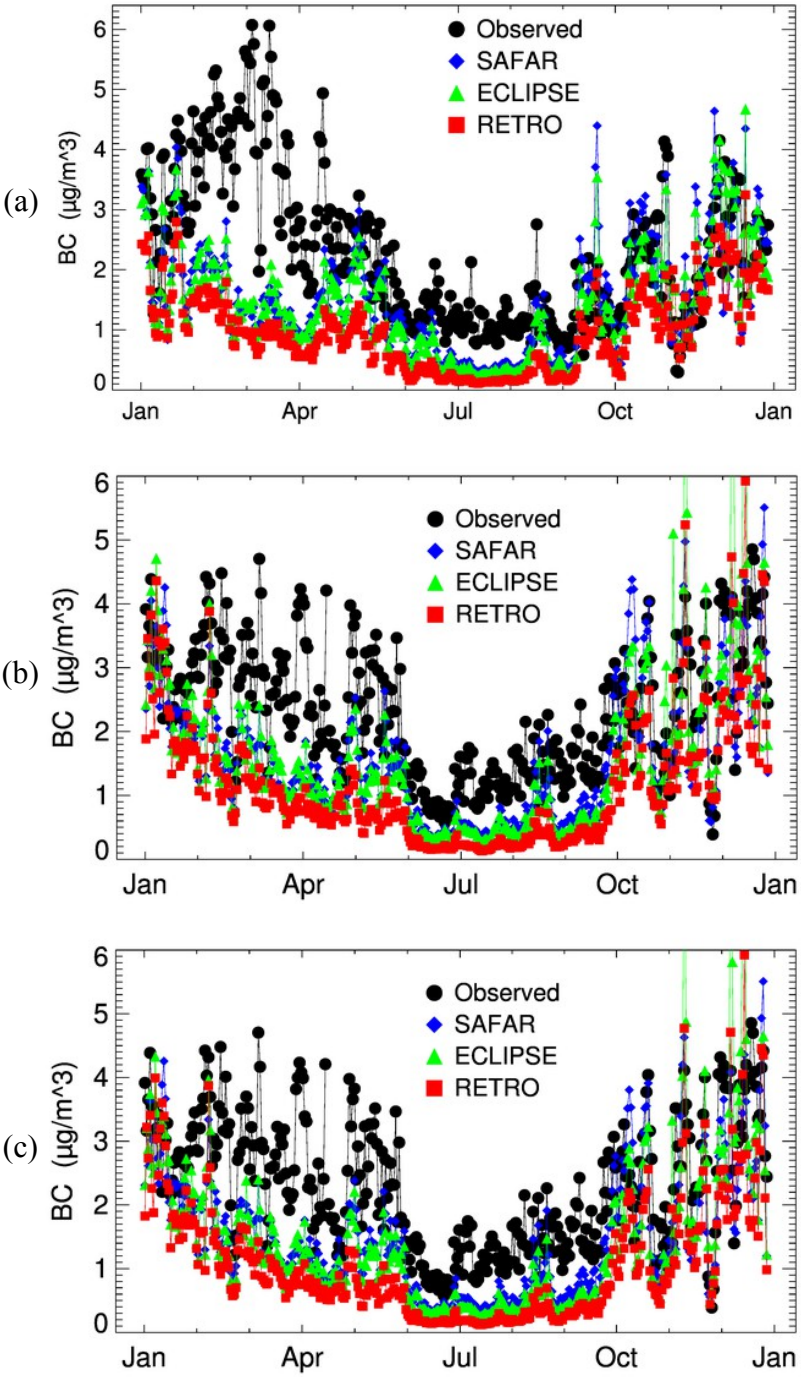

Figure 7: Comparison of observed and model estimated BC concentration. (a) 2009 without wet deposition (b) 2011 without wet deposition (c) 2011 with wet deposition.

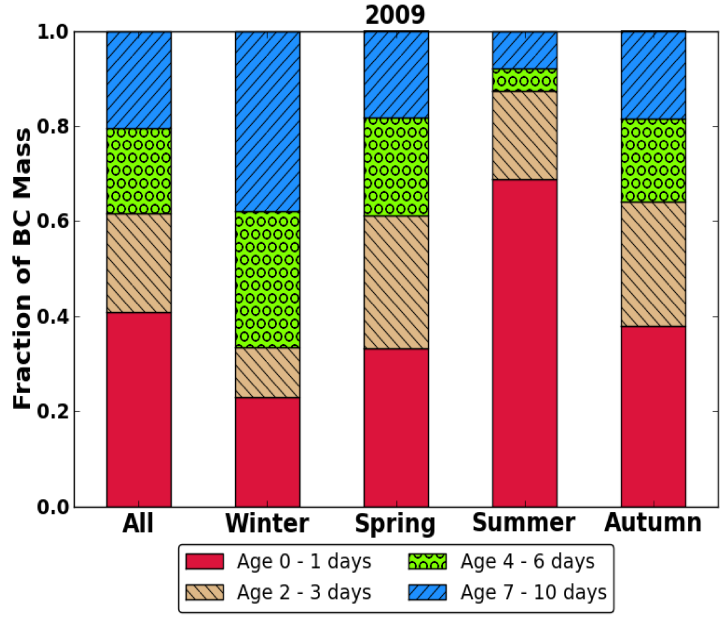

(a)

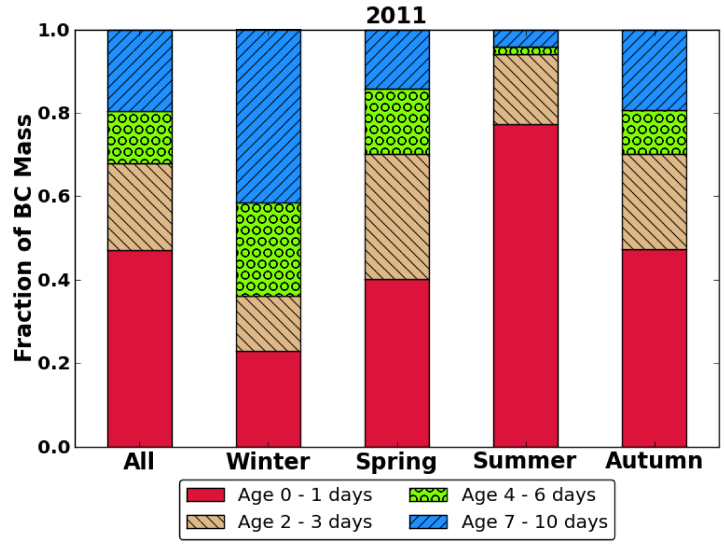

(b)

Figure 8: Fraction of simulated BC mass at Gadanki with particles of different age for year (a) 2009 and (b) 2011. Age 0-1 days represents contribution from day1 for the backward simulation. Age 2-3 days represents day2 and day3 contribution, Age 4-6 days represents day4 to day6 and Age 7-10 represents day 7 to day 10. Note that 2009 simulations are without wet-deposition whereas 2011 simulations are with wet-deposition.

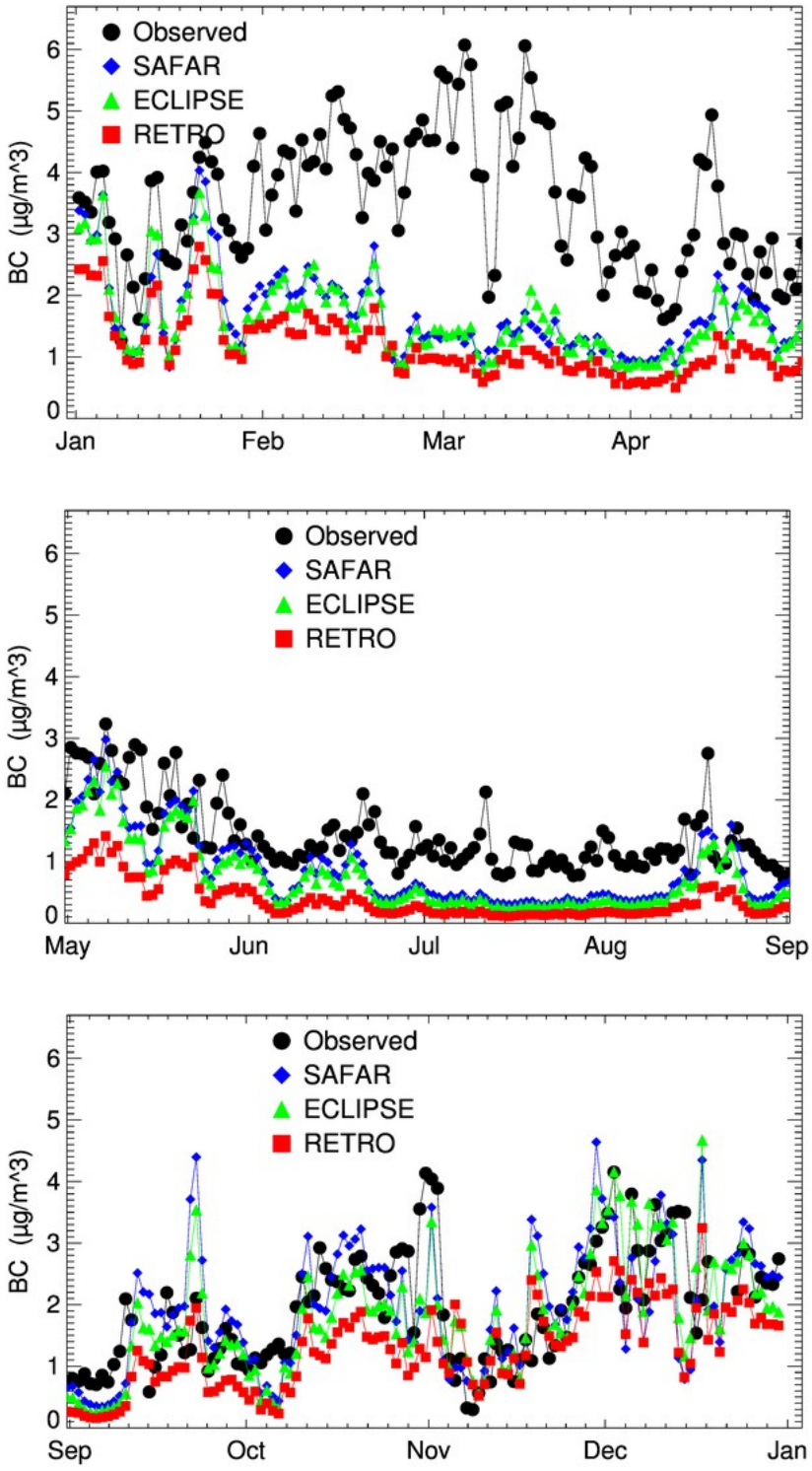

Figure 9: Same as Fig. 7a but zoomed-in for period (a) January to April (b) May to August and (c) September to December

Supporting material contains

(1) PES (Potential Emission Sensitivity) maps for each day of the year 2009. (pes_maps/PREFIX_BC_fp_YYYYMMDD.png)
(2) Map of India showing state names. (map_of_india_with_statenames.tif)
(3) Annual and seasonal average maps of fire hot spots overlaid on PES. (fire_hotspot_map_averaging-period_2009.png where averaging-period is seasons and annual).
(4) Precipitation maps from TRMM satellite for dates 9th October 2011 to 14th October 2011. (rain_trmm_YYYYMMDD.png)
(5) Plot of (negative of) exponent of wavelength of power law relating absorption coefficient to wavelength. (absorption_alpha_2009.png)
(6) README file

Supporting material can also be downloaded from following link.
http://goo.gl/OixUpN